SDC-91-122

SDC
SOLENOIDAL DETECTOR NOTES

EXTENSION OF SSC-SR-1033 APPROACH TO RADIOACTIVATION IN LHC AND SSC DETECTORS

November 4, 1991

D.E. Groom
Lawrence Berkeley Laboratory

Contribution to the *Proc. II Int. Conf. on Calorimetry in High Energy Physics,* Capri, Italy, 14–18 October 1991

SDC-91-122
04 November 1991

EXTENSION OF SSC-SR-1033 APPROACH TO RADIOACTIVATION IN LHC AND SSC DETECTORS*

D. E. Groom
Lawrence Berkeley Laboratory 50-308, Berkeley CA 94720, USA

ABSTRACT

In the SSC study of radiation levels in detectors (SSC-SR-1033), a very successful general approach was developed: The incident flux from the interaction point was described by the product of a flat pseudorapidity distribution and a transverse momentum distribution. A given effect (albedo neutrons, EM ionizing dose, ...) was studied as a function of incident particle momentum. The two functions were then combined to obtain the desired result. In the present study, the approach is extended to the radioactivation of detector components. Radioactivity in a given material is proportional to the average "star density" in hadronic cascades, as simulated in this case with FLUKA. Star density at each depth is found to scale with surprising accuracy as a power law in the incident momentum. At this stage only a "rule of thumb" is used to relate star density to activity. Results are presented for iron and lead.

1. The SSC-SR-1033 approach

The Task Force on Radiation Levels in the SSC Interaction Regions was able to approximate detector radiation levels by means of analytic functions.[1] The idea was to use a two-step approach:

1. Describe the flux incident on a detector element as a function of momentum and the position of the element.
2. Describe the effect of unit flux (one particle per unit area) on a detector element as a function of incident momentum; call this response $\phi(p)$.

The two distributions are then combined to obtain the desired response. The approach only breaks down in certain "crosstalk" situations. For example, the flux incident on a calorimeter at pseudorapidity $\eta \approx 0$ might contain significant albedo contributions from large-η regions; these are ignored. Similarly, there is an implicit approximation that the particle flux does not change significantly over the physical size of a cascade, which might not be true for a hadron calorimeter at very large η.

The production model is particularly simple, since it is known that for average events the number of particles per unit pseudorapidity interval (H) is constant in the central region to within about 10%. At the SSC this central region is expected to extend out to $|\eta| \approx 6$, or $\theta \approx 0.28°$. The distribution of the transverse component of momentum, $f(p_\perp)$, is independent of η, and so $d^2N_{ch}/d\eta\, dp_\perp \approx H\, f(p_\perp)$. Then the number of particles incident on a normal area element da at an angle θ and a distance r from the interaction point (IP) is given by

$$\frac{d^2N_{ch}}{da\, dp_\perp} = \frac{d\Omega}{da}\frac{d\eta}{d\Omega}\frac{d^2N_{ch}}{d\eta\, dp_\perp} \approx \frac{H}{2\pi r^2 \sin^2\theta} f(p_\perp)\ . \tag{1}$$

For the SSC, H is expected to be about 7.5, and the same extrapolation yields $H \approx 6.3$

* This work was supported by the U. S. Department of Energy under Contract No. DE-AC03-76SF00098.

for the LHC. The mean response of a detector element in a LHC or SSC interaction region for one (minimum bias) event then given by

$$R = \frac{H}{2\pi r^2 \sin^2\theta} \int f(p_\perp)\phi(p_\perp/\sin\theta)dp_\perp \ . \tag{2}$$

Some luck makes this integral particularly simple. In all cases studied so far, $\phi(p) \approx Ap^\alpha$. An acceptable form for the $p_\perp$ distribution is $f(p_\perp) \propto p_\perp \exp(-2p_\perp/\langle p_\perp\rangle)$. In the absence of a low-momentum cutoff (magnetic field), the integral in Eq. (2) is proportional to $\Gamma(2+\alpha)/2^\alpha$. Over the useful range $0 \le \alpha \le 1$, the same answer, within 6% in the worst case at $\alpha = 0.5$, is obtained by replacing $f(p_\perp)$ by $\delta(p_\perp - \langle p_\perp\rangle)$. It is thus sufficient to write

$$R = \frac{H\,A\,\langle p_\perp\rangle^\alpha}{2\pi r^2 \sin^{2+\alpha}\theta} = \frac{H\,A\,\langle p_\perp\rangle^\alpha}{2\pi r^2}\cosh^{2+\alpha}\eta \ . \tag{3}$$

We extrapolate existing data to estimate $\langle p_\perp\rangle = 0.60$ GeV/c at the SSC. With the same extrapolation $\langle p_\perp\rangle = 0.55$ GeV/c at the LHC.

2. Plan to include radioactivation

Cascade programs such as FLUKA[2] tally the density of nuclear interactions, or "stars," produced by hadrons above some cutoff energy, typically 50 MeV. In the "universal spectrum" approximation discussed elsewhere,[3] the rate of production of radionuclides of a given species is proportional to the star production rate in the same volume element. Some departure from this proportionality is to be expected early in the cascade, where many of the stars are produced in very high-energy collisions, but even here the departure is not thought be significant. The proportionality constant will depend on the program cutoff. The idea is that the yield per star can be established once and for all by detailed simulation, after which it can be used to relate star density to activation under arbitrary conditions in the same material.

One pitfall is that we tabulate the density of stars produced by fairly high-energy particles (mostly neutrons), whereas most of the stars are actually produced in lower-energy collisions. The lower energy neutrons have diffused somewhat further, so the activation profile is fuzzed out somewhat compared with the star density profile. As will be evident, only longitudinal smearing is relevant, and since the scale is about half of a nuclear interaction it is unlikely to be important.

Our program, then, is to describe star production as a function of depth z in typical materials and as a function of incident hadron momentum. Star density in detectors can then be calculated via Eq. (2). If we are fortunate enough to find $\phi(p,z) \propto p^\alpha$, then Eq. (3) can be used. In any case, the resulting response can be related to activation.

In this report (which has a 6-page limit), we carry this program through in detail for star production in iron and lead. The corresponding activation is only found at the level of a "rule of thumb" approximation, although the literature contains enough information for the completion of the program.[4,5]

3. Extension of the model to "star density"

FLUKA simulations of π^--induced cascades in iron and lead absorbers have been made at 9 momenta between 1 GeV/c to 500 GeV/c. In all cases the thickness was 100 cm, and the longitudinal binning was 2 cm. Transverse integrals were tablulated. (It can easily be seen that the transverse integral of such a quantity for one incident particle is the same as the density of the quantity for a uniform incident flux of one particle per unit area.) Results at two depth intervals in lead are shown in Fig. 1. The Fig. 1(b) results are typical: after the first few cm, the 10–500 GeV/c data at a given depth are very well described by a power law. At smaller depths the same thing seems to be true, but here the results are statistic-limited because of the smaller number of stars early in the cascades. In all cases, the 1 GeV/c points fall below the power-law fits. This may be real, or may be an artifact of the program. In any case it is relevant only if $\langle p \rangle$ is significantly lower than 10 GeV/c. This happens only for $|\eta| \lesssim 3$, where activation is less of a problem.

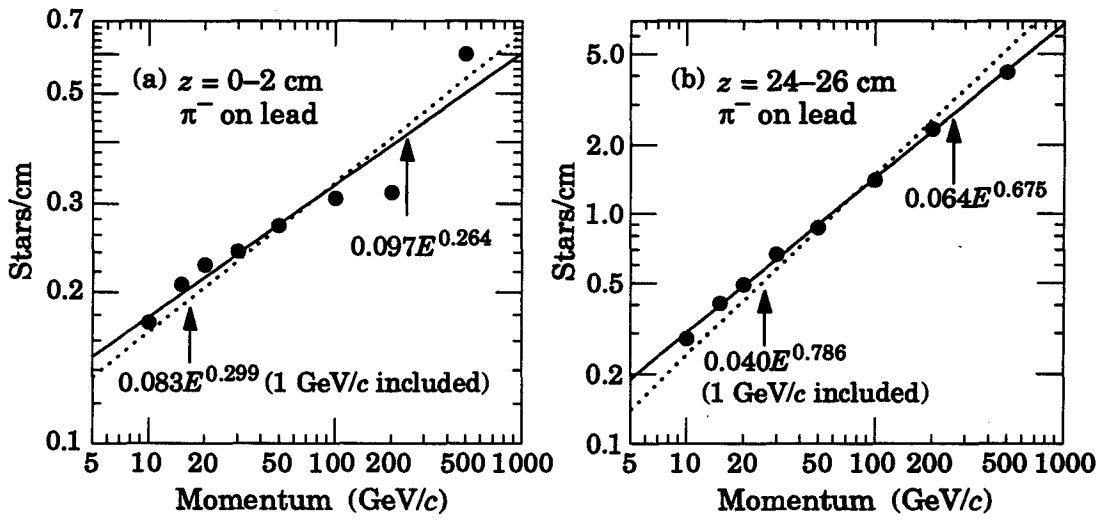

FIG. 1. Laterally integrated star density in lead per incident π^- near the surface and 25 cm deep as simulated with FLUKA. Results between 10 GeV/c and 500 GeV/c (the highest studied) are well described by power laws (solid lines), albeit statistics-limited at small depths. Results at 1 GeV/c were low in all cases, resulting in poor power-law fits (dotted lines).

Least-squares power-law fits to the function Ap^α for the 10–500 GeV/c results were used as the basis for subsequent calculations. A sampling of the results are given in Table 1. They are not very different for iron and lead, since the nuclear interaction lengths in cm are about the same for the two materials.

A worked example may be useful. We find from the table that the star density in lead is $0.097p^{0.264}$ near the surface. For a spherical lead shell "calorimeter" with an inside radius of 200 cm, Eq. (3) becomes

$$\text{Star Density} = \frac{6.3 \times 0.097 \times (0.55)^{0.264}}{2\pi \times (201\ \text{cm})^2} \cosh^{2.264}\eta = 2.06 \times 10^{-6} \cosh^{2.264}\eta\ \text{cm}^{-3}\ . \tag{4}$$

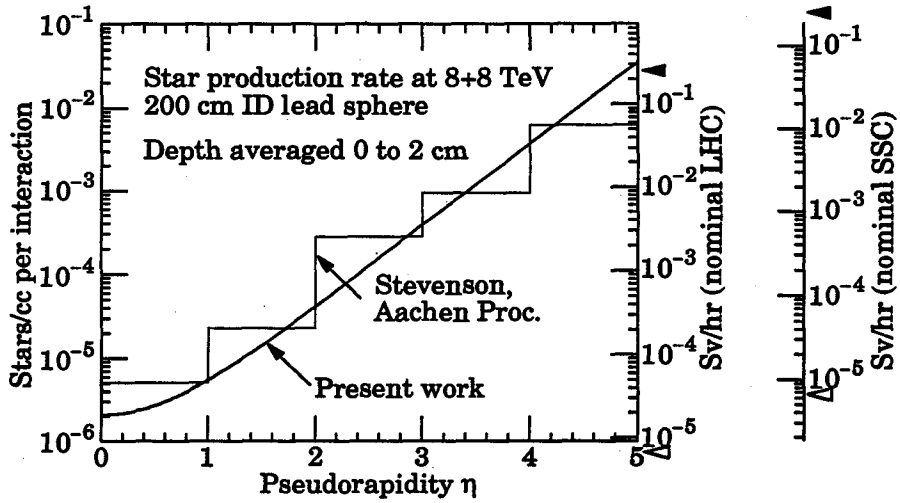

FIG. 2. Dose near the inside surface of a 2 m ID lead shell as a function of η, under nominal LHC conditions. The histogram is from a global simulation by Stevenson.[6] The right axes show conversion to dose in a scenario where a 30-day irradiation is followed by a 1-day cooldown. The open triangles indicate the CERN recommended limit to exposure (15 mSv yr^{-1} with a 2000 hr work year), and the solid triangles indicate the dose lethal to 50% of a population within 30 days of a 10 hr exposure.

Graham Stevenson reported global calculations for such a calorimeter at the the Aachen LHC workshop.[6] In Fig. 2 we compare the above result with his. As is the case at other depths, we find satisfactory agreement.

4. Relationship of star density to activation and dose

Let $f_{Z',A'}$ be the probability of producing nuclide (Z', A') per tallied star (not necessarily in that particular collision). Then, if the star *rate* per unit volume is S and the mean lifetime (halflife divided by $\ln 2$) is $\tau_{Z',A'}$, then the time derivative of the number density of this particular nuclide is

$$dN_{Z',A'}/dt = f_{Z',A'}S - N_{Z',A'}/\tau_{Z',A'} \ . \tag{5}$$

The activity $\mathcal{A}_{Z',A'}$ due to this nuclide is just $N_{Z',A'}/\tau_{Z',A'}$, and it can be seen that in equilibrium $N_{Z',A'}/\tau_{Z',A'} = f_{Z',A'}S$. In principle one would integrate Eq. (5) over the detector time history to obtain the rate for each nuclide, then sum over all the nuclides to find the total activity. Rule-of-thumb estimates can be made by (a) calculating the equilibrium activities and correcting them for decay to estimate activity after a certain cooldown period, or (b) calculating activities on the basis of some particular exposure/cooldown scenario.

The relationship between activity and dose follows from energy conservation. Consider a volume element dV inside a uniformly irradiated material with density ρ, and let E be the energy of the photons and charged particles in an average decay. Then $\mathcal{A}E\rho dV$ is the power produced in dV and deposited nearby, where $\mathcal{A}$ is the activity in Bq g^{-1}. To conserve energy, dV must also *absorb* energy at a rate $\mathcal{A}E\rho dV$, so $\mathcal{A}E$ is the dose rate ($\dot{D}$). ("Uniformly irradiated" means over the absorption distance, or a few cm.) Now suppose that all of the material to the left of dV is removed.

Since the volume element is now irradiated only from the right, it receives only half the dose. It remains only to convert this dose rate, in Bq MeV, to more conventional units such as Sv hr^{-1}. The reader can verify that the surface dose rate in Sv hr^{-1} is $2.9 \times 10^{-7} \mathcal{A}E$, with $\mathcal{A}$ in Bq and E in MeV.

5. Results

For a 50 MeV FLUKA cutoff and a star rate of 1 $cm^{-3}s^{-1}$, the equilibrium activity in iron is 0.12 Bq g^{-1}.[6] In this case $\langle E \rangle = 0.8$ MeV. Using the above conversion factor and an assumed LHC rate of 6×10^8 interactions s^{-1}, and the iron analog of Eq. (4) (where the coefficient is 1.51×10^{-6} and $\alpha = 0.257$), one obtains

$$\begin{aligned} \dot{D} &= (2.78 \times 10^{-8})(6 \times 10^8)(1.51 \times 10^{-6}) \cosh^{2.257} \eta \text{ Sv hr}^{-1} \\ &= 2.52 \times 10^{-5} \cosh^{2.257} \eta \text{ Sv hr}^{-1} \ . \end{aligned} \tag{6}$$

For historical reasons (the fixed-target era), Stevenson[6] and Höfert[7] chose 30 days at constant luminosity followed by a 1-day cooldown as the standard history. Höfert has tabulated the coefficients corresponding to the first number in Eq. (6) for a variety of materials. He obtains 1.0×10^{-8} for iron and 1.5×10^{-8} for lead. The iron coefficient is lower by a factor of 2.8 because long-lived activities such as ^{54}Mn have not had time to build up. Nonetheless, we use these coefficients in calculating the coefficients B for the expression $\dot{D} = B \cosh^{2+\alpha} \eta / r^2$, for the SSC and LHC, in iron and lead and as a function of depth, which are given in Table 1. Details are given in the caption.

As can be seen from Eq. (4), the ratio of LHC and SSC doses under nominal conditions is given by

$$\frac{\dot{D}_{LHC}}{\dot{D}_{SSC}} = \left(\frac{6 \times 10^8 \text{ s}^{-1}}{1 \times 10^8 \text{ s}^{-1}}\right) \left(\frac{6.3}{7.5}\right) \left(\frac{0.55}{0.60}\right)^{\alpha} = 5.04 \times (0.92)^{\alpha} \ . \tag{7}$$

The LHC and SSC entries in Table 1 satisfy this ratio.

Vertical scales on the right of Fig. 2 show the corresponding dose rates for the nominal SSC and LHC in Höfert's scenario. For the reasons given above, rates after a long exposure will be higher, even after a long cooldown.

For the future experiments at the LHC and SSC, this scenario is unrealistic. Exposures will be longer, and it will be impossible to access the inner detector in as short a time as a day. For purposes of reporting calculations, Stevenson proposes standardizing to a 100-day exposure followed by several fixed cooldown intervals .

How does this compare with the dose from other sources? According to Ref. 1 and its erratum, the maximum electromagnetic dose (mainly due to photons from π^0 decay) is $124 \cosh^{2.93} \eta / r^2$ Gy yr^{-1}, for r in meters. The "yr" was defined as 10^7 s, so the coefficient is equivalent to 0.045 Gy hr^{-1}(or Sv hr^{-1}). EM shower maximum occurs close enough to the surface that we can compare directly: for lead the ratio of EM dose to radioactivity dose is $600 \cosh^{0.67} \eta$. For iron it is twice as large (less radioactivity), and for an interior dose the coefficient should be divided by two. At $\eta = 5$, $\cosh^{0.67} \eta = 18$. Thus, even allowing for longer exposures and realistic integrals over cooldown times, the dose from radioactivity is smaller than the direct dose by two to four orders of magnitude. It is a personnel problem, not a radiation damage problem.

Table 1

Detector radioactivation at the LHC and SSC under nominal operating conditions (6×10^8 interactions s^{-1} at the LHC, 10^8 s^{-1} at the SSC). Other machine assumptions may be found in RPP.[8] Following Stevenson[6] and Höfert,[7] we assume a 30-day irradiation time followed by a 1-day cooldown; these doses are smaller by factors of two or three than would be obtained with longer irradiations. For solid lead or iron at a depth z given in the table, the dose, in Sv hr^{-1}, is $B \cosh^{2+\alpha} \eta / r^2$, where r is the total distance to the interaction point in meters. It is a surface dose; that is, half the dose experienced by a piece of scintillator buried in the absorber. For example: in one version of the SDC detector, the endcap starts 4.2 m from the IP. If a solid lead calorimeter section at $\eta = 3$ were cut open at a depth of 25 cm after the radiation history given above, the surface dose at would be

$$8.08 \times 10^{-6} \cosh^{2.675} 3.0/4.45^2 = 200\ \mu\text{Sv hr}^{-1}$$

Similarly, at $r = 18$ m and $\eta = 5$, the surface dose from a SSC iron calorimeter is 400 μSv hr^{-1}.

	Iron				Lead			
z (cm)	α	A	B_{LHC}	B_{SSC}	α	A	B_{LHC}	B_{SSC}
0–2	0.257	0.0708	3.65×10^{-5}	7.41×10^{-6}	0.264	0.0970	7.47×10^{-5}	1.52×10^{-5}
2–4	0.299	0.0899	4.52×10^{-5}	9.21×10^{-6}	0.352	0.1000	7.31×10^{-5}	1.50×10^{-5}
4–6	0.343	0.0985	4.83×10^{-5}	9.87×10^{-6}	0.409	0.0987	6.98×10^{-5}	1.43×10^{-5}
14–16	0.518	0.0913	4.03×10^{-5}	8.37×10^{-6}	0.557	0.0904	5.85×10^{-5}	1.22×10^{-5}
24–26	0.653	0.0663	2.70×10^{-5}	5.67×10^{-6}	0.675	0.0637	3.84×10^{-5}	8.08×10^{-6}
34–36	0.747	0.0459	1.77×10^{-5}	3.74×10^{-6}	0.783	0.0382	2.16×10^{-5}	4.58×10^{-6}
44–46	0.831	0.0305	1.12×10^{-5}	2.38×10^{-6}	0.865	0.0244	1.31×10^{-5}	2.80×10^{-6}
54–56	0.885	0.0209	7.42×10^{-6}	1.59×10^{-6}	0.932	0.0152	7.87×10^{-6}	1.69×10^{-6}
64–66	0.946	0.0135	4.62×10^{-6}	9.95×10^{-7}	1.009	0.0089	4.40×10^{-6}	9.53×10^{-7}
74–76	1.009	0.0084	2.75×10^{-6}	5.96×10^{-7}	1.076	0.0052	2.45×10^{-6}	5.33×10^{-7}
84–86	1.072	0.0051	1.61×10^{-6}	3.50×10^{-7}	1.132	0.0032	1.46×10^{-6}	3.20×10^{-7}
94–96	1.135	0.0031	9.38×10^{-7}	2.05×10^{-7}	1.217	0.0016	6.77×10^{-7}	1.49×10^{-7}

6. References

1. "Report of the Task Force on Radiation Levels in the SSC Interaction Regions," ed. by D. E. Groom, SSC Central Design Group Report SSC-SR-1033 (June 1988).
2. A. Ferrari, A. King, and G. R. Stevenson, oral tradition (1991).
3. D. E. Groom, in *Proc. of the Workshop on Calorimetry for the Superconducting Super Collider*, Tuscaloosa, Alabama, 13–17 March 1989, ed. R. Donaldson and M. G. D. Gilchriese, World Scientific (June 1990), pp. 59–75.
4. T. A. Gabriel and R. T. Santoro, Particle Accelerators **4**, 169-186 (1973).
5. T. A. Gabriel, Nucl. Instrum. Meth. **91**, 67-72 (1971).
6. G. R. Stevenson, CERN Divisional Report TIS-RP/90-18/CF; also published in *Proc. of the ECFA Large Hadron Collider Workshop*, Aachen (4–9 October 1990), CERN 90-10 (1990).
7. M. Höfert and A. Bonifas, *Measurement of Radiation Parameters for the Prediction of Dose Rates from Induced Radioactivity*, CERN Divisional Report TIS/RP/90-10/CD (1990).
8. Particle Data Group, J. Hernández *et al.*, Phys. Lett. **B239**, 1 (1990), p. III.25; see also the erratum.